J Nanopart Res
DOI 10.1007/s11051-009-9657-3

RESEARCH PAPER

# Experimental investigation into the convective heat transfer and system-level effects of $Al_2O_3$-propanol nanofluid

**Andrew D. Sommers · Kirk L. Yerkes**

Received: 11 March 2009 / Accepted: 4 May 2009


**Abstract** It has been speculated that the application of nanofluids in real systems could lead to smaller, more compact heat exchangers and reductions in material cost. However, few studies have been conducted which have carefully measured the thermo-physical properties and thermal performance of these fluids as well as examine the system-level effects of using these fluids in traditional cooling systems. In this study, dilute suspensions of 10 nm aluminum oxide nanoparticles in propanol (0.5, 1, and 3 wt%) were investigated. Changes in density, specific heat, and thermal conductivity with particle concentration were measured and found to be linear, whereas changes in viscosity were nonlinear and increased sharply with particle loading. Nanofluid heat transfer performance data were generally commensurate with that measured for the baseline. For the 1 wt% concentration, a small but significant enhancement in the heat transfer coefficient was recorded for $1800 < Re < 2800$, which is attributed to an earlier transition to turbulent flow. In the case of high particle loading (i.e. 3 wt%), the thermal performance was observed to deteriorate with respect to the baseline case. Discoloration of the fluid was also observed after being cycled at high flow rates and increased temperature.

**Keywords** Nanofluids · Aluminum oxide · Propanol · Nanoparticles · Convective heat transfer · Colloids

A. D. Sommers (✉)
Department of Mechanical and Manufacturing Engineering, Miami University, 56 Engineering Building, Oxford, OH 45056, USA
e-mail: sommerad@muohio.edu

K. L. Yerkes
Propulsion Directorate, Air Force Research Laboratory AFRL/RZP, Bldg 18A, 1950 Fifth Street, Wright-Patterson AFB, Dayton, OH 45433-7251, USA
e-mail: kirk.yerkes@wpafb.af.mil

## Introduction

The rapid proliferation of nanoparticle research over the last few years stems from the early discoveries of Choi (1995) and others who found that the seeding of a base fluid with small concentrations of nanoparticles results in an increase in the thermal conductivity of the base fluid. However, despite this recent proliferation of nanofluid research over the last few years and its potential for heat transfer enhancement, our current understanding of how nanofluids impact system components such as pumps, turbines, and heat exchangers is still currently quite limited. In fact, very little nanofluid research has been conducted in traditional heat transfer cooling systems such as those involved in the thermal management of terrestrial, naval, and aircraft propulsion and power systems. Moreover, there is still some disagreement in the

Published online: 31 May 2009

technical community regarding the methods that have been used to measure the thermal conductivity of nanofluids. Thus, a systematic, system-level investigation of the potential of nanofluids as well as a more complete understanding of their thermal-hydraulic performance is still needed.

Small concentrations of nanoparticles dispersed in liquids can substantially increase the thermal conductivity of the base fluids (Choi et al. 2001; Das et al. 2003; Ding et al. 2006; He et al. 2007). For various combinations of nanoparticle and liquids, the thermal conductivity enhancements are often far beyond the predictions of classical models for larger-sized particle suspensions, and a number of theoretical models have been proposed in the literature in an attempt to explain the heat conduction mechanisms associated with nanoparticles in liquids (Wang and Mujumdar 2007). The large enhancement of thermal conductivity has also motivated many researchers to explore the potential benefits of nanoparticle-liquid mixtures (nanofluids) in heat transfer applications during the past decade (Trisaksri and Wongwises 2007; Wen and Ding 2004). Most experimental investigations of nanofluids for single-phase laminar pipe flows have found that the convective heat transfer coefficient increases with higher particle concentrations (He et al. 2007; Heris et al. 2007; Lee and Mudawar 2007; Pak and Cho 1998). The enhancement of laminar-flow forced convection was more pronounced at the entrance region (Heris et al. 2007; Pak and Cho 1998). Similarly, increased convective heat transfer coefficients were found for turbulent flows (Koo and Kleinstreuer 2004; Xuan and Li 2003; Nguyen et al. 2007; Yang et al. 2005). The convective heat transfer enhancement by nanoparticles for laminar and turbulent flows tends to increase with Reynolds number, and the magnitude is generally beyond that of thermal conductivity, with at least one exception (Prasher et al. 2006).

Among other properties of nanofluids, the viscosity increases significantly with increasing nanoparticle concentration. However, certain studies have suggested an insignificant pressure drop penalty for pipe flows for both laminar and turbulent flows (Koo and Kleinstreuer 2004; Xuan and Li 2003; Nguyen et al. 2007). In contrast, a recent experiment with a micro-channel heat sink has resulted in a notable increase in pressure drop with an increasing concentration of alumina nanoparticles, while the friction factor was nearly unaffected (Pak and Cho 1998). Rheological studies of nanofluids found both Newtonian behaviors (Ding et al. 2006; Putra et al. 2003) and shear-thinning behaviors (He et al. 2007; Koo and Kleinstreuer 2004; Xuan and Li 2003). Despite these early promising results, little work has been conducted to assess the effects of nanoparticles on system components such as pumps, flowmeters, gages, and valves. Recent studies, however, have also suggested that by accounting for linear particle aggregation, most of the thermal conductivity enhancement data reported in the data can be explained by classic medium theories for composite materials. These studies also point out that the particle loading needed to achieve this affect also increases the viscosity, which renders its merits for flow-based cooling questionable (Keblinski et al. 2008; Ghandi 2007). A critical review of recent research in the area of nanofluid convective heat transfer states both this promise and concern (Wang and Mujumdar 2007).

Despite this wealth of nanofluid research and the potential for heat transfer enhancement, our current understanding of how nanofluids impact system components and affect overall system performance is still quite limited. More specifically, the long-term chemical and mechanical effects of nanoparticle additives on flow lines, pumps, and heat exchangers are still largely unknown, and the claims of anomalous thermo-physical property enhancement are not completely unexplained. If nanofluids are to be applied to real systems, these outstanding issues must be properly addressed.

The objective of this study was to provide a better understanding of the effects of nanoparticles on system level thermal performance and system components and to provide demonstrative evidence of either the benefits or the detriments derived from seeding a heat transfer fluid with nanoparticles. Thermo-physical properties were measured, and convective heat transfer characteristics determined for dilute concentrations of a $Al_2O_3$/propanol nanofluid in a counter flow, single-pass convective loop. The impact of this nanofluid on the overall system thermal performance and components was assessed. In this study, nanoparticle concentrations of 0.5, 1.0, and 3.0 wt% were examined. Collected data were compared against well-known correlations found in

the literature, and multiple methods of measurement were used to improve the overall accuracy of the measured fluid properties.

## Experimental method

### Flow loop construction

The convective heat transfer experiments were conducted in a single-pass, counter flow loop consisting of four major sections: thermal conditioning, flow conditioning, test section, and reservoir as shown in Fig. 1. The nanofluid flowed through a 3/4-inch ID copper pipe. The test section consisted of an 18-inch long copper block heated by hot water. Heat rates of 50, 100, 150, 200, and 250 W were supplied to the copper block by varying the temperature of the water. Turbulators were used to ensure that the water was well mixed, and copper thermal grease was used to ensure that there was good thermal contact between the pipe and the block. The average energy balance between the test fluid and the water loop was 7.9%.

The temperature of the propanol at the inlet of the test section was maintained at 30 °C using a Lytron liquid-to-liquid brazed plate heat exchanger where water was used as the secondary cooling fluid. A 39-inch long entrance region was used to condition the flow and ensure fully developed conditions in the test section. Both turbulent and laminar flow conditions were explored. A 1-L accumulator was used to allow for the expansion and contraction of the working fluid. The total charge of the system was approximately 2.5 L.

Type-T thermocouple probes calibrated against an AFRL-traceable high-precision platinum RTD were used to measure the inlet and outlet temperatures of the propanol and water in the test section, and six type-T thermocouples attached to the copper pipe with thermal paste were used to measure the wall surface temperature as shown in Fig. 2. Flow turbulators and 90° elbows were used to ensure that the outlet fluid was well mixed prior to measurement. The uncertainty in the measured temperature difference used to calculate the convective coefficient was ±0.05 °C with 95% confidence. An OMEGA PX2300 low-differential pressure transducer with an uncertainty of ±0.0625 psid was used to measure the pressure drop across the test section. The volumetric flow rate of the fluid was varied from 0.5 to 2.5 GPM and measured using an oval gear, positive displacement flowmeter (OMEGA) with an uncertainty of ±0.5% of the reading. Once thermal equilibrium was

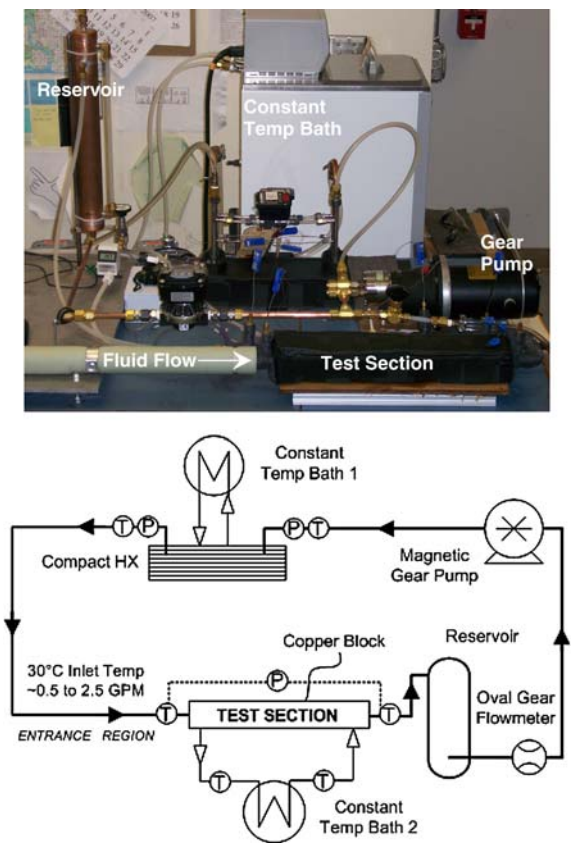


**Fig. 1** Photograph of the experimental test loop and schematic

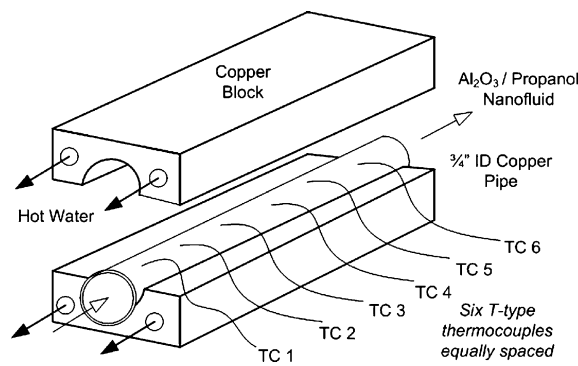


**Fig. 2** Schematic of the test section and surface-mounted thermocouples

established, heat transfer data were acquired for a period of 2 min and averaged.

## Nanofluid properties

The nanofluid under investigation in this study was $Al_2O_3$/propanol. The nanofluid was purchased from NanoAmor© in a pre-mix form containing 20 wt% aluminum oxide nanoparticles (gamma phase) with an average particle size of 10 ± 5 nm. A proprietary surfactant (<1 wt%) was used to improve dispersion of the particles. Nanofluid weight concentrations of 0.5% and 1.0% were then prepared by dilution of the pre-mix fluid with 99.95% pure propanol (reagent grade). Propanol was chosen as the base fluid for a couple of reasons. First, propanol has a low thermal conductivity (i.e., $k_{\text{propanol, 30 °C}} = 0.14$ W/mK) comparable to that of PAO which is used in military applications for engine lubrication and cooling. Therefore, similar enhancements might be expected for the two fluids. It was also hypothesized that if a thermal enhancement existed, it would be more pronounced in propanol than in more traditional working fluids which possess higher thermal conductivity [i.e., water, ethylene glycol (EG), etc.]. Second, because propanol has a rather low boiling point (i.e., $T_{\text{boil}} \approx 82$ °C), two-phase heat transfer experiments were planned if the single-phase heat transfer data warranted continued investigation.

### *Density measurement*

The density of both the nanofluid and base fluid was measured at room temperature using two methods and compared. In the first method, a hydrometer was used to measure the specific gravity of a fluid sample. In the second method, a fluid sample of known volume was taken and then weighed on a high-precision balance (±0.001 g). Data collected using these two methods were then averaged and can be seen in Fig. 3a. A nearly linear relationship between density and particle concentration can be observed.

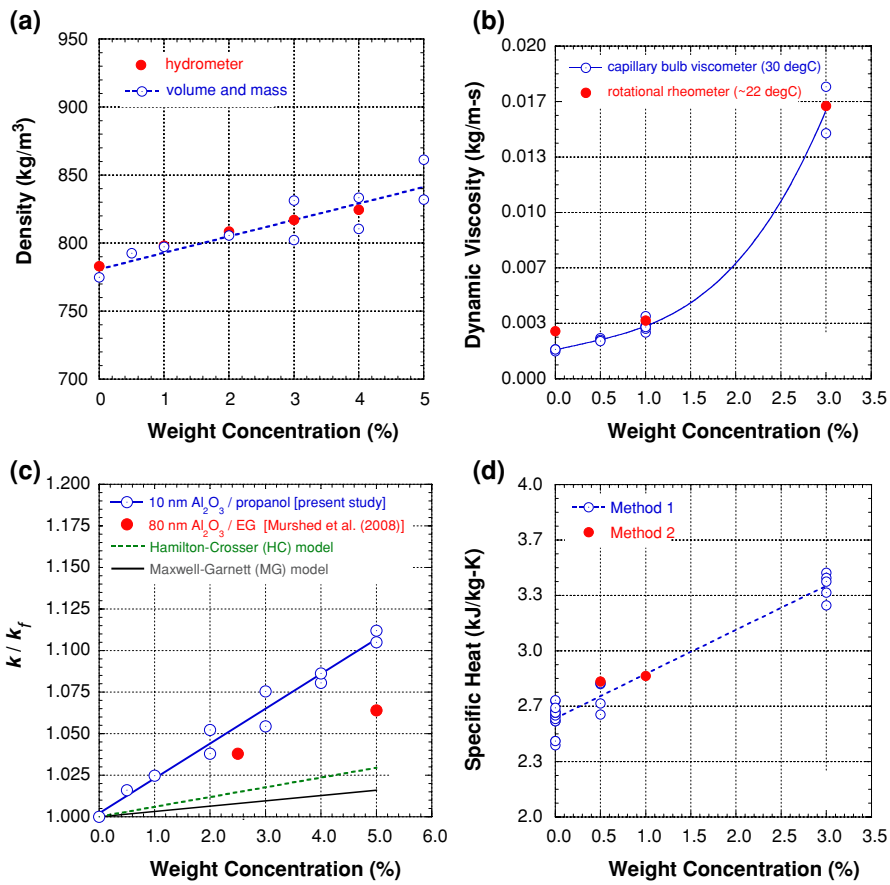


**Fig. 3** Thermophysical property information for the $Al_2O_3$/propanol nanofluid

Good agreement (<1.8%) was observed between the two methods for nanofluid concentrations ≤4 wt%. At higher concentrations of nanoparticles, however, it was observed that measurements taken using the hydrometer became increasingly less accurate.

*Viscosity measurement*

The measurement of viscosity proved to be the most difficult and most elusive so two different techniques were employed. First, a capillary bulb viscometer was used which proved to be accurate for low particle loading. It could also be used in conjunction with an isothermal bath and thus could be used to measure the kinematic viscosity of the fluid at 30 °C. Second, an Anton Paar RheolabQC rheometer was used, which could only measure the viscosity at room temperature, but had the advantage of being less sensitive to the nanoparticle concentration. Unlike the other thermo-physical properties, viscosity exhibited non-linear behavior with concentration with the viscosity increasing sharply for concentrations >1.0 wt%. These data can be seen in Fig. 3b. A non-Newtonian shear-thinning behavior was observed for the nanofluid.

*Thermal conductivity measurement*

The thermal conductivity $k$ was measured at room temperature (i.e., 22 °C) using the transient hot-wire method. Using this method, the thermal conductivity for propanol was found to be 0.17 W/mK which is slightly higher than the value generally accepted for propanol at room temperature. The difference is attributed to uncertainties in the measurement technique and the fact that the propanol used in this measurement was only 99.9% pure. The observed percent enhancement in thermal conductivity—for example, 10% for a 5 wt% concentration—was linear with concentration and was comparable to what has been reported by others in the literature for alumina nanoparticles in base fluids such as EG and engine oil (Murshed et al. 2008). These measured $k$ values were slightly higher than Murshed et al. (2008), but this can be attributed to the smaller particle size and lower base fluid thermal conductivity. (The thermal conductivity of propanol is approximately two times lower than the thermal conductivity of EG.) Overall, the thermal conductivity enhancement due to the $Al_2O_3$ nanoparticles, however, was relatively small due primarily to the low-fluid temperatures investigated in this study.

These data were also compared to two traditional $k$ models for composites: the Hamilton–Crosser (HC) model for dilute suspensions of spherical particles and the Maxwell-Garnett (MG) model for composite systems where the matrix thermal conductivity is much smaller than the particle thermal conductivity. Both models were observed to under predict the measured thermal conductivity data (see Fig. 3c). The HC model is given by

$$\frac{k}{k_m} = 1 + \frac{3\phi(k_p - k_m)}{k_p + 2k_m - \phi(k_p - k_m)}, \tag{1}$$

where $k_m$ is the matrix thermal conductivity, $k_p$ is the particle thermal conductivity, and $\phi$ is the volume fraction (Hamilton and Crosser 1962). Although the HC model has been successfully applied to large particle composite systems, the model does have its limitations. For example, in the limit where $k_p >> k_m$ and for low $\phi$, Eq. 1 predicts that $k/k_m$ should be three times the volume fraction irrespective of particle geometry and size. The MG model, which accounts for particle size and interfacial thermal resistance, is given by

$$\frac{k}{k_m} = \frac{(1+2\alpha) + 2\phi(1-\alpha)}{(1+2\alpha) - \phi(1-\alpha)}, \tag{2a}$$

$$\text{where } \alpha = 2R_b k_m / d \tag{2b}$$

and $R_b$ is the Kapitza resistance and $d$ is the particle diameter (Prasher 2005; Prakash and Giannelis 2007). (The MG model predictions shown in Fig. 3c assume an average particle size of 10 nm and a Kapitza resistance of $0.8 \times 10^{-8}$ K m$^2$ W$^{-1}$ which is representative of $Al_2O_3$ in water.) In considering Eq. 2, it is interesting to note that the interfacial resistance of nano-sized particles should be more significant than for micron-sized particles which would tend to decrease $k/k_m$, not increase it. Thus, the inclusion of interfacial effects is insufficient for explaining the enhancements in thermal conductivity that were observed here and have been reported elsewhere in the literature (Choi et al. 2001; Das et al. 2003; Ding et al. 2006; He et al. 2007). These observations, which have led researchers to suggest other physical mechanisms such as micro-convection due to Brownian diffusion, have also raised questions regarding the

applicability of the hot-wire technique for nanofluid thermal conductivity measurement. It should be pointed out, however, that both of these models (i.e., Hamilton–Crosser and Maxwell-Garnett) are based in effective medium theory that assumes well-dispersed particles in a fluid matrix. If particle aggregates are formed in the fluid resulting in particle chains or clusters, the predicted thermal conductivity would be significantly higher as was observed.

*Specific heat measurement*

The measurement of specific heat was performed using multiple methods to reduce the uncertainty associated with its determination. In the first method, an energy balance was performed around the brazed plate heat exchanger such that

$$\mathrm{cp}_{\mathrm{nf}} = \frac{\dot{m}_{\mathrm{H_2O}} \mathrm{cp}_{\mathrm{H_2O}} \Delta T_{\mathrm{H_2O}}}{\dot{m}_{\mathrm{nf}} \Delta T_{\mathrm{nf}}}, \quad (3)$$

where $\dot{m}_{\mathrm{H_2O}}$ refers to the mass flow rate of the water stream, $\dot{m}_{\mathrm{nf}}$is the mass flow rate of the nanofluid, $\Delta T_{\mathrm{H_2O}}$ is the water-side temperature difference between the inlet and outlet, $\Delta T_{\mathrm{nf}}$ is the nanofluid-side temperature difference between the inlet and outlet, and $c_{\mathrm{p,H_2O}}$ is the heat capacity of the water. This method, however, assumed perfect heat transfer between the two streams and as a result often under-predicted the specific heat of the nanofluid by 5–7%. In the second technique, the specific heat value of the nanofluid was adjusted until the average energy balance for all tests matched the average energy balance determined during baseline testing ($n = 34$). The specific heat value calculated using this method was found to be a bit higher and more consistent with expectations. These data are plotted in Fig. 3d.

*Nephelometric turbidity measurement*

The quality of the nanofluid dispersion was also monitored using a Micro100 turbidimeter from HF Scientific® with a tungsten filament light source. For these tests, a cuvette of the 3 wt% $Al_2O_3$/propanol nanofluid was inserted into the test chamber and then left undisturbed. The nephelometric turbidity units (NTUs) were recorded and found to be unchanged over the period of performed testing—a time period exceeding 30 days (see Fig. 4). A blank cuvette was indexed prior to monitoring and found to possess a value of 3.85 NTUs which is small compared to the measured turbidity of the nanofluid. During the monitoring period, the turbidity was observed to increase slightly but may be due to the settling of alumina nanoparticles from above into the test region increasing the relative opacity of the fluid. It should be noted, however, that this increase in turbidity lies just outside of the experimental uncertainty. Slightly more rapid settling was observed for the 1 wt% $Al_2O_3$/nanofluid nanofluid as compared to the 3 wt% nanofluid which may be due to lower concentrations of the proprietary surfactant. Regardless, these findings suggest that this nanoparticle dispersion is rather stable, and relatively little to no settling of the alumina nanoparticles would be expected during testing in the flow loop. The uncertainty in these measurements was ±2% of the reading or 14 NTUs.

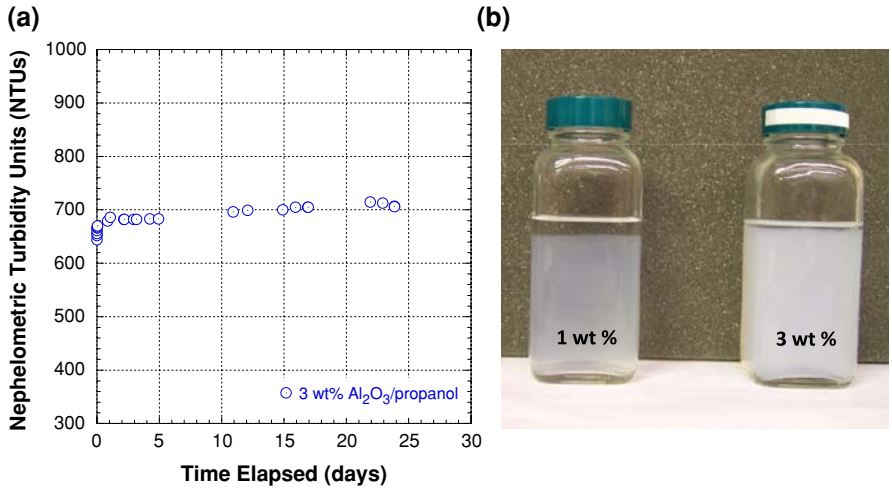


**Fig. 4** **a** Turbidity measurements performed on the 3 wt% nanofluid suggest very gradual particle settling. **b** Images of the 1 and 3 wt% nanofluid approximately 2½ weeks after preparation confirm these data although some settling can be observed

## Data reduction procedure

Energy balances were monitored to ensure fidelity of all measured data. For 82% of the data points reported, the maximum energy transfer difference was 10.7% while the remaining 18% of the data had energy balances between 10.7% and 17.2% as can be seen in Fig. 5. The energy balance discrepancies are largely attributable to the uncertainties in measuring the water-side heat transfer rate which typically range from 5% to 7%. The log mean temperature difference (LMTD) method was then utilized to interpret the thermal performance of the fluid and determine the convective heat transfer coefficient. The convective coefficient was found using the water-side heat transfer rate, $Q_{\text{water}}$, and calculating the thermal resistances associated with convection on the water side (i.e., $R_{\text{water,conv}}$) and conduction through the copper pipe (i.e., $R_{\text{wall,cond}}$) according to

$$Q_{\text{water}} = \text{UA} \cdot \text{LMTD}, \tag{4a}$$

where

$$\text{LMTD} = \frac{\left(T_{\text{water,in}} - T_{\text{nf,out}}\right) - \left(T_{\text{water,out}} - T_{\text{nf,in}}\right)}{\ln\left(T_{\text{water,in}} - T_{\text{nf,out}}\right) / \left(T_{\text{water,out}} - T_{\text{nf,in}}\right)}, \tag{4b}$$

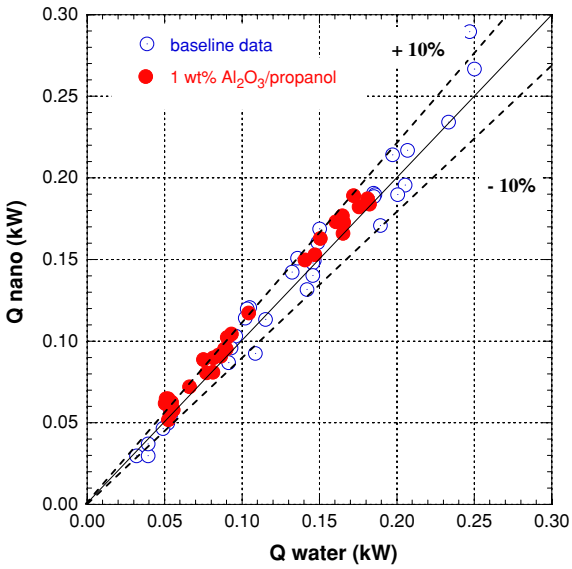


**Fig. 5** Energy balances for the baseline and nanofluid data were typically <10%

$$\text{UA} = \frac{1}{\left(R_{\text{water,conv}} + R_{\text{wall,cond}} + R_{\text{nf,conv}}\right)}, \tag{4c}$$

and

$$R_{\text{nf,conv}} = \frac{1}{\left(2\pi r_{\text{i}} L h_{\text{nf}}\right)}. \tag{4d}$$

In these equations, UA is the overall thermal conductance, $T_{\text{water,in}}$ is the test section water inlet temperature, $T_{\text{water,out}}$ is the water outlet temperature, $T_{\text{nf,in}}$ is the nanofluid inlet temperature, and $T_{\text{nf,out}}$ is the nanofluid outlet temperature. The water-side thermal resistance and pipe conduction resistance were found to be small compared to the thermal resistance associated with forced convection on the nanofluid side, $R_{\text{nf,conv}}$. Thus, the reported nanofluid convection coefficient, $h_{\text{nf}}$, in this study was determined using:

$$h'_{\text{nf}} = \frac{k_{\text{pipe}} \cdot Q_{\text{water}}}{\left(r_i\left(2\pi k_{\text{pipe}} L\left(T_{\text{wall}} - T_{\text{nf,avg}}\right) - Q_{\text{water}} \cdot \ln\left({}^{r_{\text{o}}}/_{r_{\text{i}}}\right)\right)\right)}, \tag{5}$$

where $T_{\text{wall}}$ is the average pipe surface temperature, $T_{\text{nf,avg}}$ is the bulk fluid temperature, $k_{\text{pipe}}$ is the thermal conductivity of the copper pipe, $L$ is the test section length, and $r_{\text{o}}$ and $r_{\text{i}}$ are the outer and inner pipe radius, respectively. The measured convection coefficient was compared with the convection resistance found using the Gnielinski (1976) correlation and Colebrook (1939) correlation for fully developed, turbulent flow conditions and the Sieder and Tate (1936) correlation for laminar flow with a combined entry length. Those equations are shown here for completeness such that

$$\text{Nu}_{\text{SiederandTate}} = 1.86\left(\frac{\text{Re}_D \cdot \text{Pr}}{L/D}\right)^{1/3}\left(\frac{\mu}{\mu_{\text{s}}}\right)^{0.14} \tag{6}$$

and

$$\text{Nu}_{\text{Gnielinski}} = \left(\frac{f}{8}\right)\left(\frac{\left(\text{Re}_D - 1000\right) \cdot \text{Pr}}{1 + 12.7(f/8)^{1/2}\left(\text{Pr}^{2/3} - 1\right)}\right), \tag{7a}$$

where

$$f = 1 \Big/ \left(1.5635 \cdot \ln(\text{Re}_D/7)\right)^2 \tag{7b}$$

where Nu is the Nusselt number, $\text{Re}_D$ is the Reynolds number, Pr is the Prandtl number, $f$ is the friction

factor, $\mu$ is the fluid viscosity, and $\mu_s$ is the fluid viscosity evaluated at the wall surface temperature.

## Results and discussion

The thermal hydraulic performance of the 2-propanol base fluid was measured before and after the addition of the $Al_2O_3$ nanoparticles. Tests were performed for nanoparticle concentrations of 0.5, 1.0, and 3.0 wt%. All tests were performed for an inlet temperature of 30 °C unless otherwise noted. In order to assess the pressure drop penalty associated with the addition of the 10 nm $Al_2O_3$ nanoparticles, the nanofluid was tested over a wide range of volumetric flow rates.

The results in Fig. 6 reveal a pressure penalty associated with the nanofluid even under low particle loading conditions (i.e. 1 wt% or 0.2 vol%) that varies between 400% for $Re_D = 1000$ and 600% for $Re_D = 2000$. The additional pressure drop (i.e., 0.2–1.0 psi) generated by the increase in fluid viscosity over this range of Reynolds numbers was significant. However, it should be noted that the incremental pumping power needed to overcome this deficit would be less than approximately 1.1 W when using the 1 wt% $Al_2O_3$/propanol nanofluid. When plotted versus volumetric flow rate, the pressure drop penalty is observed to be more pronounced at low flow rates. This is attributed to the rheology of the nanofluid—specifically its shear-thinning behavior. Thus, at higher flow rates and therefore higher rates of fluid shearing strain, the increase in the viscous shear stress is diminished and the overall pressure drop penalty decreases.

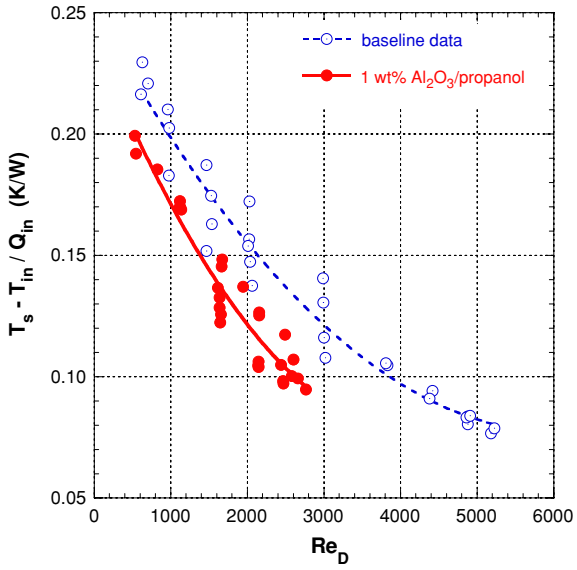


**Fig. 7** Normalized heat transfer rate versus Reynolds number for the 1 wt% $Al_2O_3$/propanol nanofluid

The heat transfer rate was then normalized by the difference between the fluid inlet temperature and the test section surface temperature and plotted versus the Reynolds number is shown in Fig. 7. These data which do not explicitly reveal the effect that the fluid properties have on the overall thermal performance show a heat transfer augmentation for the 1 wt% nanofluid. In order to investigate the mechanism behind this enhancement, the normalized heat transfer was then plotted versus the fluid thermal conductivity ratio as shown in Fig. 8. These data suggest that the observed augmentation in heat transfer was the result of the enhanced thermophysical properties of

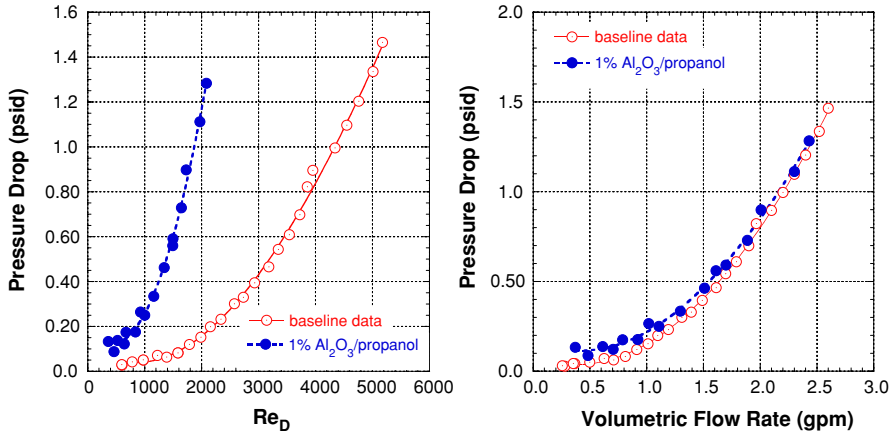


**Fig. 6** Pressure drop data for the 1 wt% $Al_2O_3$/propanol nanofluid

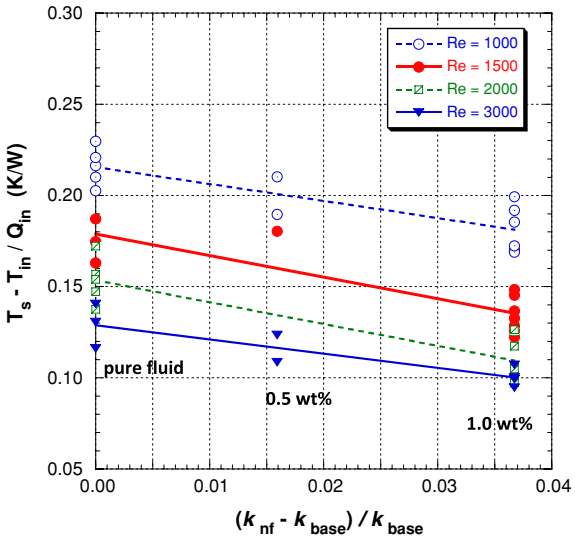


**Fig. 8** Normalized heat transfer rate versus fluid thermal conductivity ratio

the $Al_2O_3$/propanol nanofluid and not some other mechanism such as Brownian motion-induced nano-convection, liquid layering, or other interfacial effects. For example, in Fig. 7 for $Re_D = 2000$, the normalized heat transfer ratio, $(T_s - T_{inlet})/Q$, decreases from $\sim$0.16 to 0.12 K $W^{-1}$ between the baseline and 1 wt% $Al_2O_3$/propanol nanofluid. In Fig. 8, for $Re_D$ also equal to 2000, the normalized heat transfer rate decreases by the same amount between the baseline and 1 wt% case. Thus, the change in heat transfer was due almost exclusively to the increase in the fluid thermal conductivity. Perhaps, more importantly, these plots which show system thermal performance do not require the use of Brownian diffusion to explain thermal-fluid behavior.

Next, the effect of the $Al_2O_3$ nanoparticles on the convective heat transfer coefficient was explored. The baseline (i.e., pure propanol) convective heat transfer coefficient data were observed to agree well with the Gnielinski (1976) correlation for fully-developed turbulent flow and the Sieder and Tate (1936) correlation for a combined entry length, laminar flow as shown in Fig. 9a. The close agreement of these data with published correlations further corroborates the integrity of the data and the low observed energy balance differences between the test fluid stream and the hot water stream in Fig. 5. For the 0.5 wt% $Al_2O_3$/propanol nanofluid over the range of testable Reynolds numbers $500 < Re_D < 3400$, there was no measurable difference in the thermal behavior of the fluid versus the pure propanol (see Fig. 9b). (Note: Because of the increase in fluid viscosity with the addition of the nanoparticles, it was difficult to achieve $Re_D > 3500$ without changing the experimental setup of the flow loop.)

For the 1.0 wt% $Al_2O_3$/propanol nanofluid, there was also no measurable difference in the convective heat transfer coefficient of the fluid for $Re_D < 2000$. For $2000 < Re_D < 3000$, a small but significant enhancement of $\sim$15–20% was observed. The uncertainty in these calculated values of the heat transfer coefficient was typically <8.2% with the maximum uncertainty not exceeding 16%. This enhancement was repeatable and was later observed again using a new sample of 1 wt% $Al_2O_3$/propanol nanofluid. Two different mechanisms have been proposed to explain this enhancement. First, it is believed that the addition of the nanoparticles may have actually served to precipitate an earlier transition from laminar to turbulent flow which would mean higher Nusselt numbers. Thus, the transition region might exhibit slightly improved heat transfer as compared to the baseline fluid, but this enhancement would only be expected to occur within a very narrow region of Reynolds numbers. Once the base fluid transitioned to turbulent flow, similar heat transfer performance would be expected. A second mechanism which might explain this small observed enhancement lies with the rheology of the fluid. Because the nanofluid is shear-thinning and the shear rate is highest near the wall, better fluid flow performance should be realized near the wall. Thus, the non-uniform distribution of the viscosity field across the tube cross-section (and/or the possibility of a reduced boundary layer) might also explain this enhancement. However, when the heat transfer data were non-dimensionalized as $Nu/Pr^{1/3}$ and plotted versus Reynolds number as shown in Fig. 9c, no enhancement was manifest. Thus, the ability of this nanofluid to enhance convective heat transfer remains dubious.

Studying the thermal performance of the nanofluid at high mass flow rates was difficult due to the increase in fluid viscosity and the limitations imposed by the pump. However, a limited quantity data were collected by increasing the fluid inlet temperature to 50 °C to reduce the apparent viscosity of the fluid and removing the brazed plate heat exchanger from the

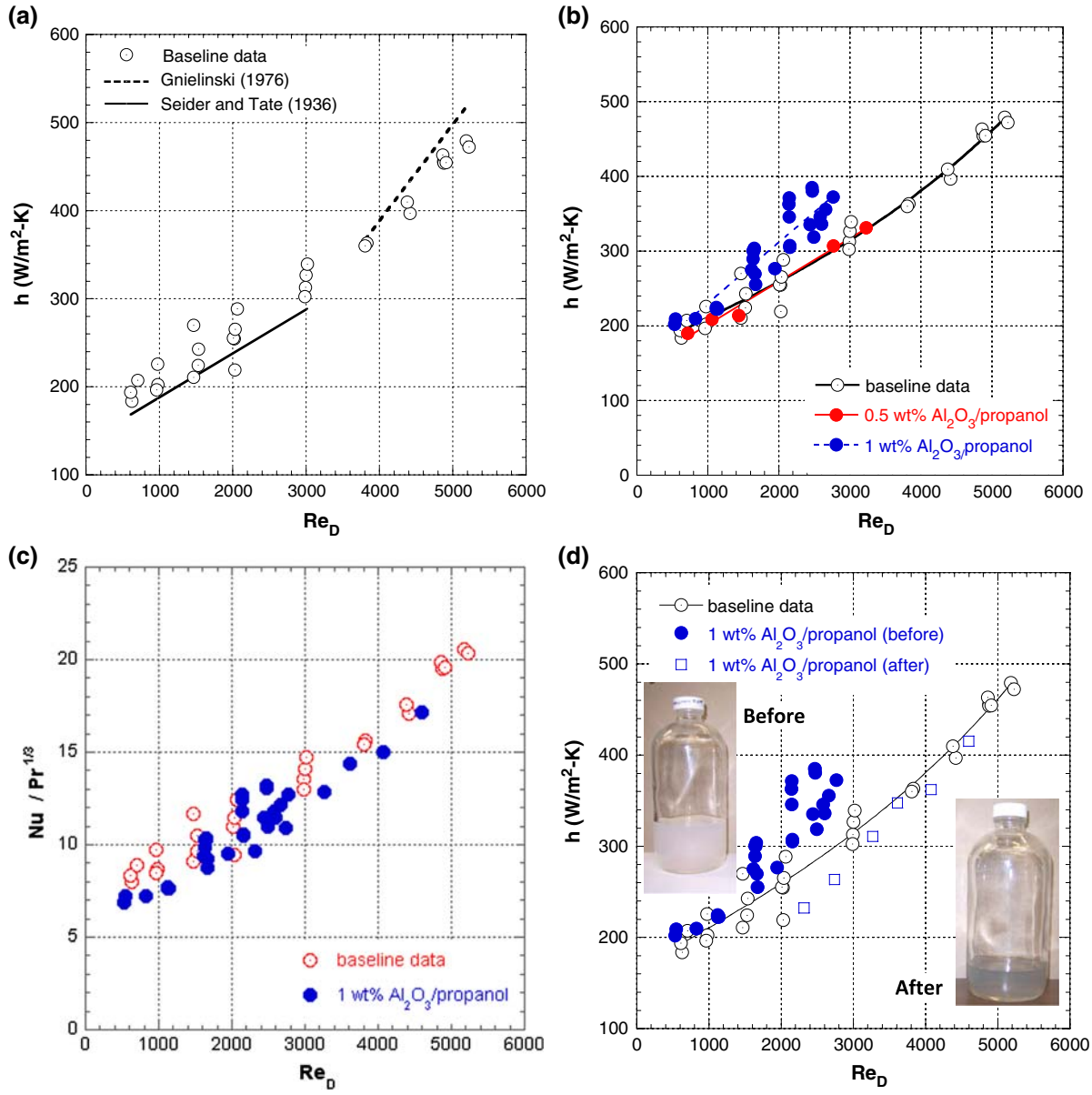


**Fig. 9** Thermal performance data for the baseline, 0.5 wt%, and 1 wt% $Al_2O_3$/propanol nanofluid

flow loop. For these experiments, data were first collected at the highest achievable flow rate (i.e., $Re_D = 4600$) and then the flow was incrementally reduced. During these experiments (performed at elevated temperature and higher flow rates), significant discoloration of the nanofluid was observed. Although a little discoloration of the fluid had been observed earlier, the discoloration became more pronounced during these tests. The thermal performance of the fluid during these tests was similar to the base fluid thermal performance, and it was observed that the thermal performance deteriorated with increasing discoloration of the fluid. (This can be seen in Fig. 9d for the final data that were collected for $Re_D < 3000$.) To help identify the source, samples of the 1 wt% $Al_2O_3$/propanol nanofluid were taken before and after discoloration and examined using X-ray powder diffraction (XRD) spectroscopy and Fourier transform infrared (FTIR) spectroscopy. The fluid was centrifuged, and the

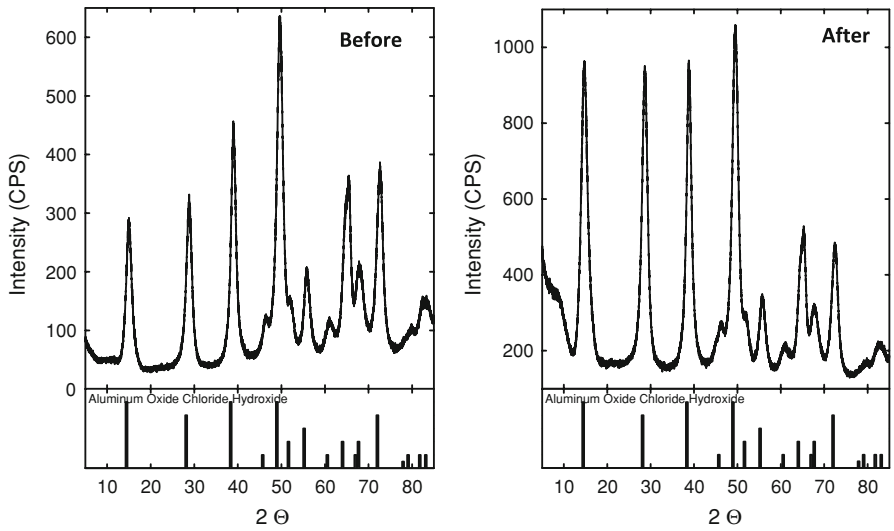


**Fig. 10** XRD spectra for the 1 wt% $Al_2O_3$/propanol nanofluid before and after flow loop cycling

liquid and solid portions were examined separately. The results shown in Fig. 10 for the XRD exhibited peaks characteristic of aluminum oxide and a hydroxide group as expected. However, the data from both the XRD and FTIR analyses showed very little difference in the "before" and "after" samples making it difficult to determine the source of the discoloration but suggesting that the optical change was due to trace contaminants. Although the reason for the discoloration is not known, it is conjectured that nano-abrasion of a softer material in the flow loop may be responsible since the Vickers hardness value of $Al_2O_3$ is very high (approx. 2500 kg $mm^{-2}$). Possible sources include the polyphenylene sulfide (PPS) oval gears in the flow meter or an amorphous barrier coating deposited on a part by plasma, inert gas atomization, or high-velocity spraying. This explanation is corroborated by the observation that the discoloration was exacerbated at elevated temperatures and volumetric flow rates.

## Conclusions

The thermal-hydraulic performance of dilute suspensions of 10 nm aluminum oxide nanoparticles in propanol was explored. Changes in density, specific heat, and thermal conductivity with particle concentration were measured and found to be linear. Changes in viscosity, however, were found to be nonlinear and increased sharply with particle loading. Nanofluid heat transfer performance data were also measured and were generally commensurate with the baseline data. For $Re_D < 3000$, the heat transfer coefficient for pure propanol ranged from 200 to 330 W $m^{-2}$ $K^{-1}$, whereas typical values for the 1 wt% $Al_2O_3$/propanol nanofluid ranged from 200 to 380 W $m^{-2}$ $K^{-1}$. At the same time, the pressure drop was found to increase from 400% to 600% for the 1 wt% $Al_2O_3$/propanol nanofluid for $Re_D < 2100$. Discoloration of the nanofluid was also observed after being cycled at high flow rates and increased temperature for long periods of time which may be the result of nano-abrasion occurring in the loop. Based on these results, the use of an $Al_2O_3$/propanol nanofluid for thermal enhancement does not appear to be justified. Moreover, it suggests that rather than using nanoparticles to enhance heat transfer performance, conventional methods such as increasing the heat transfer surface area and thinning out the thermal boundary layer might be used instead to achieve the same thermal-fluid behavior.

**Acknowledgments** The authors are grateful to Augusta Runyon, Aaron Veydt, Cheryl Castro, Christopher Bunker, and Barbara Harruff for their help and expertise in completing this study.

## References

Choi SUS (1995) Enhancing thermal conductivity of fluids with nanoparticles. In: Proceedings of the 1995 ASME International Mechanical Engineering Congress and Exposition, San Francisco, CA, USA

Choi SUS, Zhang ZG, Yu W, Lockwood FE, Grulke EA (2001) Anomalous thermal conductivity enhancement in nanotube suspensions. Appl Phys Lett 79:2252–2254. doi:10.1063/1.1408272

Colebrook CF (1939) Turbulent flow in pipes with particular reference to the transition region between the smooth and rough pipe laws. J Inst Civil Eng 11:133–156

Das SK, Putra N, Roetzel W (2003) Pool boiling characteristics of nano-fluids. Int J Heat Mass Transfer 46:851–862. doi:10.1016/S0017-9310(02)00348-4

Ding Y, Alias H, Wen D, Williams RA (2006) Heat transfer of aqueous suspensions of carbon nanotubes (CNT nanofluids). Int J Heat Mass Transfer 49:240–250. doi:10.1016/j.ijheatmasstransfer.2005.07.009

Ghandi KS (2007) Thermal properties of nanofluids: controversy in the making? Curr Sci 92:717–718

Gnielinski V (1976) New equations for heat and mass transfer in turbulent pipe and channel flow. Int Chem Eng 16:359–368

Hamilton RL, Crosser OK (1962) Thermal conductivity of heterogeneous two-component systems. Ind Eng Chem Fundam 1:187–191. doi:10.1021/i160003a005

He Y, Jin Y, Chen H, Ding Y, Cang D, Lu H (2007) Heat transfer and flow behavior of aqueous suspensions of $TiO_2$ nanoparticles (nanofluids) flowing upward through a vertical pipe. Int J Heat Mass Transfer 50:2272–2281. doi:10.1016/j.ijheatmasstransfer.2006.10.024

Heris SZ, Esfahany MN, Etemad SGh (2007) Experimental investigation of convective heat transfer of $Al_2O_3$/water nanofluid in circular tube. Int J Heat Fluid Flow 28:203–210. doi:10.1016/j.ijheatfluidflow.2006.05.001

Keblinski P, Prasher R, Eapen J (2008) Thermal conductance of nanofluids: is the controversy over? J Nanopart Res 10:1–9. doi:10.1007/s11051-007-9352-1

Koo J, Kleinstreuer C (2004) A new thermal conductivity model for nanofluids. J Nanopart Res 6:577–588. doi:10.1007/s11051-004-3170-5

Lee J, Mudawar I (2007) Assessment of the effectiveness of nanofluids for single-phase and two-phase heat transfer in micro-channels. Int J Heat Mass Transfer 50:452–463. doi:10.1016/j.ijheatmasstransfer.2006.08.001

Murshed SMS, Leong KC, Yang C (2008) Investigations of thermal conductivity and viscosity of nanofluids. Int J Therm Sci 47:560–568. doi:10.1016/j.ijthermalsci.2007.05.004

Nguyen CT, Roy G, Gauthier C, Galanis N (2007) Heat transfer enhancement using $Al_2O_3$-water nanofluid for an electronic liquid cooling system. Appl Therm Eng 27:1501–1506. doi:10.1016/j.applthermaleng.2006.09.028

Pak BC, Cho YI (1998) Hydrodynamic and heat transfer study of dispersed fluids with submicron metallic oxide particles. Exp Heat Transf 11:151–170. doi:10.1080/08916159808946559

Prakash M, Giannelis EP (2007) Mechanism of heat transport in nanofluids. J Comput Aided Mater Des 14:109–117

Prasher R (2005) Thermal conductivity of nanoscale colloidal solutions (nanofluids). Phys Rev Lett 94:025901. doi:10.1103/PhysRevLett.94.025901

Prasher R, Song D, Wang J, Phelan P (2006) Measurements of nanofluid viscosity and its implications for thermal applications. Appl Phys Lett 89:133108. doi:10.1063/1.2356113

Putra N, Roetzel W, Das SK (2003) Natural convection of nano-fluids. Heat Mass Transf 39:775–784. doi:10.1007/s00231-002-0382-z

Sieder EN, Tate GE (1936) Heat transfer and pressure drop of liquids in tubes. Ind Eng Chem 28:1429–1436

Trisaksri V, Wongwises S (2007) Critical review of heat transfer characteristics of nanofluids. Renew Sustain Energy Rev 11:512–523. doi:10.1016/j.rser.2005.01.010

Wang X-Q, Mujumdar AS (2007) Heat transfer characteristics of nanofluids: a review. Int J Therm Sci 46:1–19. doi:10.1016/j.ijthermalsci.2006.06.010

Wen D, Ding Y (2004) Experimental investigation into convective heat transfer of nanofluids at the entrance region under laminar flow conditions. Int J Heat Mass Transfer 47:5181–5188. doi:10.1016/j.ijheatmasstransfer.2004.07.012

Xuan Y, Li Q (2003) Investigation on convective heat transfer and flow features on nanofluids. J Heat Transfer 125:151–155. doi:10.1115/1.1532008

Yang Y, Zhang ZG, Grulke EA, Anderson WB, Wu G (2005) Heat transfer properties of nanoparticle-in-fluid dispersions (nanofluids) in laminar flow. Int J Heat Mass Transfer 48:1107–1116. doi:10.1016/j.ijheatmasstransfer.2004.09.038